Revista Brasileira de Ensino de Física, vol. 43, e20200437 (2021)
www.scielo.br/rbef
DOI: https://doi.org/10.1590/1806-9126-RBEF-2020-0437

Articles

Chua's oscillator: an introductory approach to chaos theory

Alexandre Sordi*[1]

[1]Universidade Tecnológica Federal, Departamento de Engenharia Mecânica, Londrina, PR, Brasil.

Received on October 14, 2020. Accepted on November 04, 2020.

The purpose of this article is to build an introductory approach to chaos theory from the Chua' oscillator for students of mathematics, physics and engineering. The Chua' circuit is one of the simplest dynamic systems that produce irregular behavior. Despite its simplicity, this oscillating circuit is a very useful device for studying basic principles of chaos theory. This study begins with the definition of equilibrium points, this is done in a graphic and analytical way. The analysis of the stationary solution of differential equations system allows to show the occurrence of pitchfork bifurcation. The eigenvalues are calculated and the trajectories of the Chua' oscillator are analyzed, then the occurrence of Hopf bifurcation is demonstrated. Period-doubling cascade are observed using phase portrait and orbit diagram. Finally, sensitivity to initial conditions is studied by calculating Lyapunov exponents.

Keywords: Non-linear oscillator, chaos theory, attractors.

1. Introduction

Irregular behavior is present in almost every aspect of life, whether natural or artificial. This refers to those that are between the rigidly predictable and the purely random. Systems in this gap are known as chaotic and have some distinguishing properties: nonlinearity, sensitivity to initial conditions, long-time unpredictability. The apparently random time evolution meant that this mode of behavior was often mininterpreted as noise. A pioneer of what is now known as chaos theory was Lorenz [1] with his study of a small-scale model of the atmosphere. Lorenz observed that the trajectories from the solution of the respective autonomous differential equation system exhibited extreme sensitivity to tiny changes of the initial conditions. Since then the theory has been developed in such a way that it has been discovered that its tools could be used to understand various types of systems. It was soon explored in various areas, such as engineering, chemistry, communication, computing, biology, medicine, finance, electronics, etc. [2]. One of the most notable nonlinear systems is the Chua oscillating circuit due to its simplicity, robustness and diverse dynamics. It was elaborated by Leon Chua at Waseda University in Japan in 1983 [3] on the assumption that a chaotic autonomous circuit should exhibit at least two unstable equilibrium points. Until then, there were only two autonomous dynamic systems that were generally accepted as chaotic: Lorenz's and Rössler's. The first with three points and the second with two unstable equilibrium points. Chua then identifying this mechanism as the main cause of chaos in those systems systematically elaborated a circuit with such attributes. Its methodology in the theory of nonlinear circuits was effective, extensive computational simulations of the circuit demonstrated the occurrence of chaotic attractors in its behavior [4], the same was confirmed experimentally [5]. Since its invention the circuit has been well studied, its dynamics has become well known due to numerous works produced. In addition to the electronics area itself, other applications of the Chua's oscillator have already been considered such as music and acoustics [6]; in chemistry by introducing a chaotic model of electrons into atoms and an analogy between synchronization of two chaotic systems and covalent bonding [7], and also exploring the similarity between bifurcation diagrams and the spectrum of atoms [8]. It is also possible to find mechanical and electromechanical systems whose dynamics are governed by the same differential equations of the Chua's circuit [9]. More recently in [10] the analogy between the memristive Chua's circuit and Newton's second law is demonstrated. The simplest example of a mechanical memristor can be seen in [11], where the coefficient of viscous friction depends on the history of the relative velocity between its terminals. This article analyzes the Chua's oscillator using basic principles of chaos theory. Section 2 shows the electrical circuit and the differential equations for the dynamical analysis. Basic concepts of chaos analysis methodology are covered in Section 3 for Chua's oscillator study. Equilibrium points are obtained and classified. The occurrence of Hopf and period-doubling bifurcations, double scroll strange attractors and sensitivity to initial conditions are demonstrated.

* Correspondence email address: ydros911@gmail.com.

2. The Chua's Circuit

Figure 1 illustrates the canonical Chua's circuit [12], which is so termed because it is associated with every possible qualitative dynamics of a wide variety of piecewise-linear differential equations in R^3. It consists of a simple network of passive linear components such as resistors R_0 and R, capacitors c_1 and c_2, and an L inductor. In addition to these also an active nonlinear element NR, commonly called Chua's diode, whose driving-point characteristic can be represented by a family of continuous piecewise functions, such as that in Figure 1(b).

Although a very simple system, the Chua's circuit can exhibit extremely diverse dynamics. Thus, with the appropriate assignment of parameters, it is possible to observe period doubling, intermittency, and torus breakdown routes to chaos [13]. The experimental implementation of the Chua's circuit mainly depends on the nonlinear element assembly. There are several configurations in the literature. For more detail on the one that uses op-amps, for example, the reading of the works is indicated [14, 15]. Applying Kirchoff's laws to circuit of Figure 1(a), the following system of differential equations is obtained:

$$\begin{aligned}\frac{de_1}{dt} &= \frac{1}{c_1}\left[\frac{1}{R}(e_2 - e_1) - e_1\frac{1}{R_{NR}} - i(e_1)\right]\\ \frac{de_2}{dt} &= \frac{1}{c_2}\left[\frac{1}{R}(e_1 - e_2) + i_3\right]\\ \frac{di_3}{dt} &= -\frac{1}{L}\left[e_2 + R_0 i_3\right]\end{aligned} \tag{1}$$

Where the piecewise-linear function that represents the characteristic of the non-linear resistor is replaced by a sigmoid function with a voltage transition e_t:

$$i(e_1) = k\tanh\left(\frac{e_1}{e_t}\right)$$

The electric flux is $\phi = \int e dt$, so:

$$\frac{d\phi_1}{dt} = e_1, \frac{d\phi_2}{dt} = e_2 \tag{2}$$

We can write equation (1) and (2) in dimensionless form by making the following variables exchange:

$$\begin{aligned}x &= \frac{e_1}{e_t}, y = \frac{e_2}{e_t}, z = \frac{i_3 R}{e_t},\\ u &= \frac{\phi_1}{e_t c_1 R}, w = \frac{\phi_2}{e_t c_2 R}, \tau = \frac{t}{c_2 R}\\ a &= \frac{k}{e_t R}, b = \frac{R}{R_{NR}}, \alpha = \frac{c_2}{c_1},\\ \beta &= \frac{c_2 (R)^2}{L}, \epsilon = \frac{c_2 R R_0}{L}\end{aligned}$$

Soon,

$$\begin{aligned}\frac{dx}{d\tau} &= \alpha[y - x - (bx + i(x))]\\ \frac{dy}{d\tau} &= x - y + z\\ \frac{dz}{d\tau} &= -\beta y - \epsilon z\end{aligned} \tag{3}$$

Where:

$$\begin{aligned}\frac{du}{d\tau} &= x\\ \frac{dw}{d\tau} &= y\\ i(x) &= a\tanh(\psi x)\end{aligned}$$

since the ψ value defines how abrupt the voltage transition is. The system of equations (3) is the same as that seen in [16], where it is shown to have dynamic behaviour very similar to the original differential equations of the Chua's circuit. For simulation of dynamics by numerical solution the following parameter values can be used, namely, $a = -0.428$, $b = -0.614$, $\alpha = 9.0$, $\beta = 15.0$, $\epsilon = 0.125$, $\psi = 2.0$.

3. Stability and Chaos Analysis

To find the stationary or equilibrium solutions of the differential equations system one must calculate the fixed

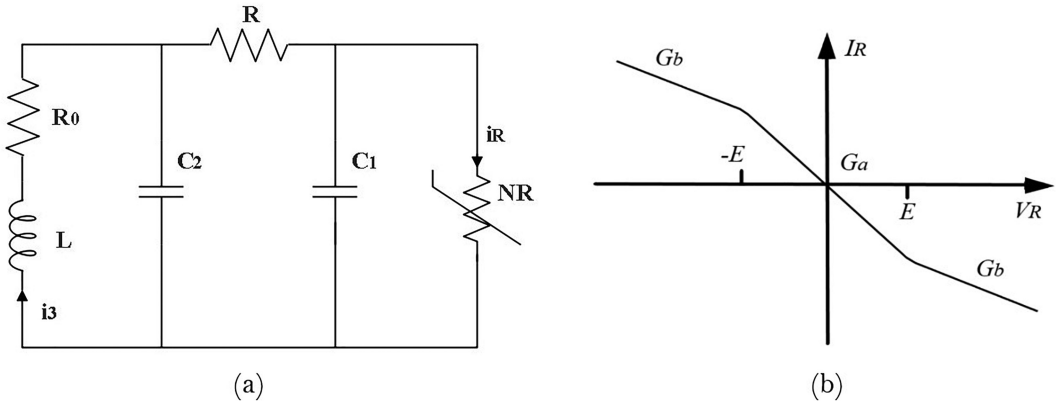

Figure 1: (a) Canonical Chua's circuit. (b) Driving-point characteristic of the nonlinear resistor.

 DOI: https://doi.org/10.1590/1806-9126-RBEF-2020-0437

points which represent stagnation sites. These points are characterized by a stable or unstable equilibrium, and are therefore defined as follows:

$$0 = \alpha[y - x - (bx + i(x))]$$
$$0 = x - y + z$$
$$0 = -\beta y - \epsilon z$$

Which is equivalent to opening the circuit of Figure 1(a) at capacitances c_1 and c_2, and a short circuit at inductance L to find the stationary solution. It is quick to conclude that the system has the following solution:

$$i = -x\left(\frac{\beta}{(\beta+\epsilon)} + b\right) \tag{4}$$

Equilibrium points can be found by taking the intersection of equation (4) with non-linear sigmoid function $i = i(x)$. By setting the β, ϵ parameters, and making a variation of the b parameter the qualitative dynamics analysis is performed as follows.

Figure 2 shows the graphs of $i = -x(\frac{\beta}{(\beta+\epsilon)} + b)$, and $i = a\tanh(\psi x)$, their intersections correspond to the fixed points. Note that as $|b|$ decreases the line becomes steeper. So for $|b| \to 0$ there is only one fixed point at the origin, this point is characterized by stable equilibrium since $dx/dt > 0$ on the left and $dx/dt < 0$ on the right of origin. There is a critical value b_c where the slopes of the two friction functions are equal, that is,

$$b_c = -\left(2a + \frac{\beta}{(\beta+\epsilon)}\right) \tag{5}$$

For this value there is a pitchfork bifurcation that is common in physical systems that have symmetry, such as the Chua's oscillator, the origin at $x* = 0$ is slightly stable. Finally for $|b| > |b_c|$ the origin becomes unstable and a symmetrical pair of stable equilibrium points

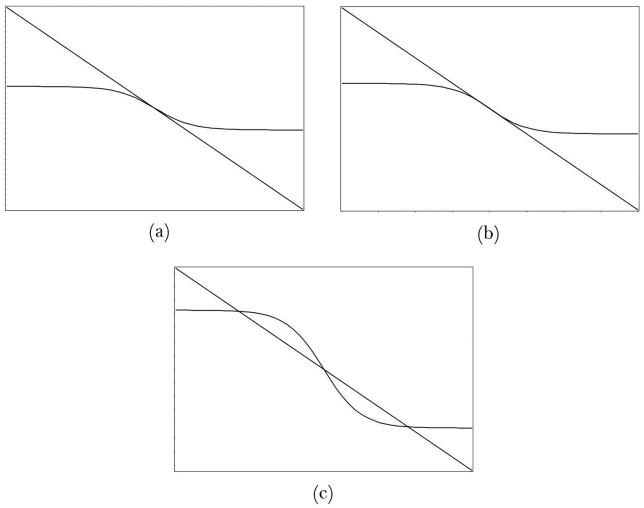

Figure 2: (a) $|b| < b_c$. (b) $|b| = b_c$. (c) $|b| > b_c$

arises, $P+, P-$. These two new symmetrical fixed points corresponding to left and right-Chua configuration, the oscillator can move right or left.

The stability of the fixed points can be completely specified by the Jacobian matrix $\mathbf{J}$ eigenvalues:

$$\begin{bmatrix} -\alpha(1 + b + 2a(1 - \tanh(2x_*)^2)) & \alpha & 0 \\ 1 & -1 & 1 \\ 0 & -\beta & -\epsilon \end{bmatrix}$$

That is, identifying the zeros of the characteristic polynomial. For the Chua's oscillator in general $\mathbf{J}$ has a real eigenvalue γ and a pair of conjugated complex eigenvalues $\sigma \pm j\omega$. The solution of $d\mathbf{r}/dt = \mathbf{J}r(t)$ can be written in terms of the sum of two components, $\mathbf{r}(t) = \mathbf{x}_r(t) + \mathbf{x}_c(t)$, where:

$$\mathbf{x}_r(t) = A\exp(\gamma t)\mu$$
$$\mathbf{x}_c(t) = 2B\exp(\sigma t)$$
$$[\cos(\omega t + \theta)\eta_r - \sin(\omega t + \theta)\eta_i]$$

Where η_r, and η_i are the eigenvectors associated respectively to $\sigma \pm j\omega$, and define a complex eigenplane $\mathbf{E}^c$. The μ is the real eigenvector defined by $\mathbf{J}\mu = \gamma\mu$. A, B, θ are constants that depend on the initial conditions. As is done in [15] the dynamics analysis is then performed by assuming three distinct regions: central region, $D_0(|e_1| \leq e_t)$, and outer regions $D_1(e_1 < -e_t), D_{-1}(e_1 > e_t)$. Keeping all other parameters constant, when $|b| = \frac{5}{25}$ the equilibrium points in the outer regions respectively, $(P+, P-)$, have the following eigenvalues:

$$\gamma_1 \approx -2.293$$
$$\sigma_1 \pm j\omega_1 \approx -0.014 \pm j2.721$$

While the equilibrium point in D_0 region,

$$\gamma_0 \approx 1.151$$
$$\sigma_0 \pm j\omega_0 \approx -0.886 \pm j2.764$$

Depending on its initial state the system may remains around either outer equilibrium point, $P+$ or $P-$. It is observed that the real eigenvalue $\gamma_1 < 0$, and the real part of complex conjugate $\sigma_1 < 0$. A negative real eigenvalue σ_1 causes trajectories to be squeezed into the complex eigenplane $E^c(P\pm)$ itself. The solution component in $\mathbf{E}^c$ spirals toward to equilibrium point along this plane, and the component in μ tends asymptotically to $(P\pm)$. When the two components are added, it is shown that a trajectory beginning near the stable real eigenvector $\mu(P\pm)$ above the complex eigenplane moves toward $E^c(P\pm)$ along a helix of exponentially decreasing radius. Since the two components decrease exponentially in magnitude, the trajectory is quickly flattened into $E^c(P\pm)$, where it goes towards equilibrium point along the complex eigenplane. The graphs shown below

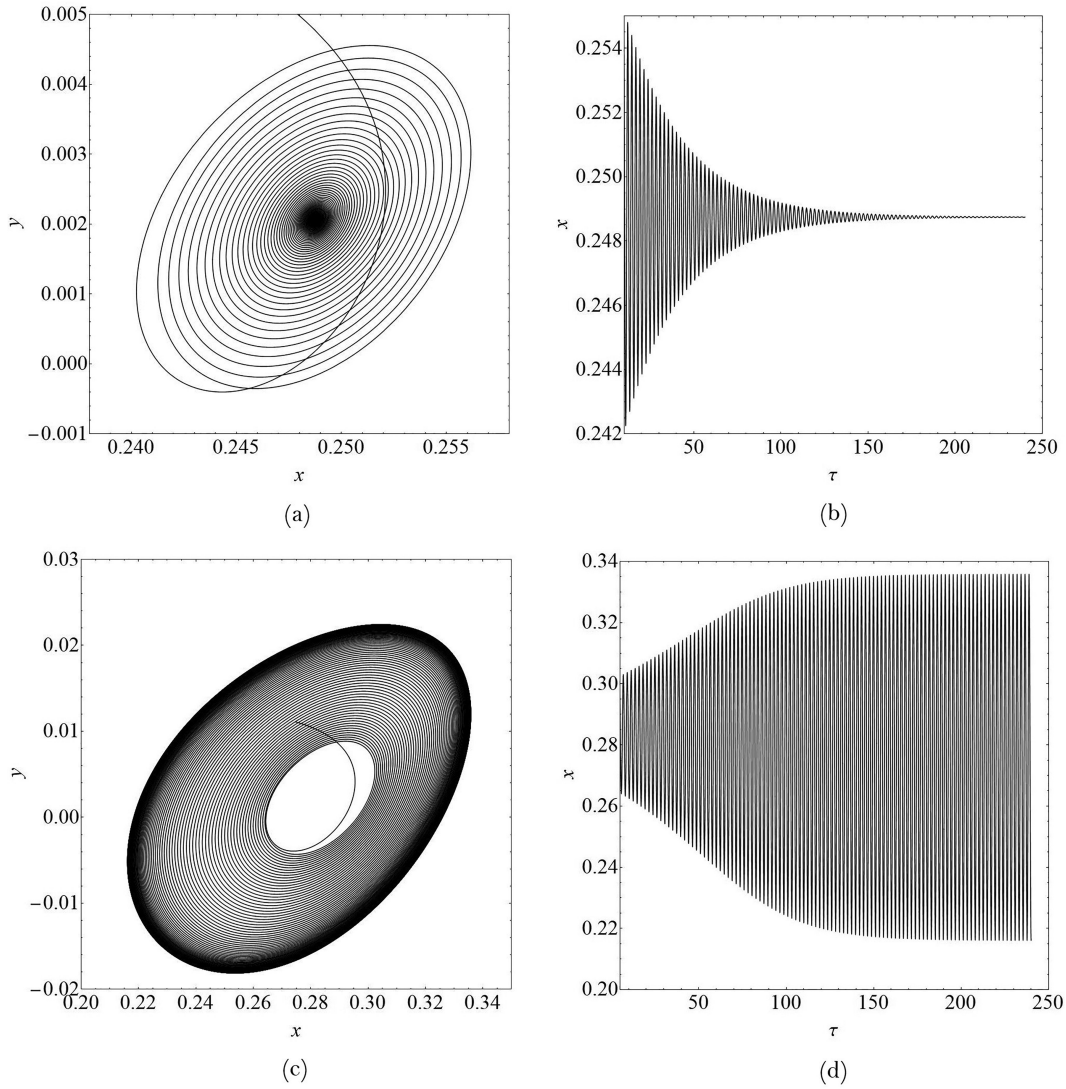

Figure 3: (a) Dynamics of the D_1 region. (b) Velocity oscillations of m_1. (c), (d) Limit cycle due to Hopf bifurcation.

are the result of numerical calculations using the fourth-order Runge-Kutta method with fixed step size of 0.001. In the Figure 3(a) the oscillation of e_1 decays towards the equilibrium point $P+$. The electrical oscillations are damping since x shows an exponential decay. The decay rate of e_1 dynamics can be slowed down by increasing the value of $|b|$, and thereafter a critical value b_c for which the oscillations make themselves growing in amplitude. Thus, the previous stability is lost as the σ_1 of the complex conjugate goes through zero and reverses its signal to positive. The system is said to have a Hopf bifurcation. The real eigenvalue of $P+$ remains negative, so the trajectories converges toward to eigenplane $\mathbf{E}^c$. The Figure 3(c) shows the simulation for $|b| = \frac{5}{23}$ where the trajectory becomes an unstable spiral circumscribed by an approximately elliptical stable limit cycle. Therefore, after a transient the oscillations stabilize for a limit cycle of period 1 (Figure 3(d)). After a certain value of $|b|$ period-doubling occurs. Thereafter the limit cycle circles point $P+$ twice until it is completed, i.e. the trajectory of a period 2 orbit takes approximately twice as long to fully evolve, as shown in Figure 4(b). As one further increases, a series of period-doubling bifurcations is observed: period 4 (Figure 4(c)), period 8 (Figure 4(d)). The series continues for period 16, 32 until it reaches an infinite period orbit where chaos and the strange attractor or spiral of the Chua's oscillator are observed (Figure 4(e)). Because the nonlinearity associated with the Chua's oscillator is symmetric, every attractor that exists in the D_1 and D_0 region has a copy in the D_{-1} and D_0 regions. Such counterpart can be observed by further increasing the parameter $|b|$ (Figure 5). Note that spiral-Chua and your mirror image form a composite attractor commonly called double-scroll Chua strange attractor.

It is useful to show all possible dynamic behaviours for a parameter value range, such as b for example. To perform this task we use the orbit diagram [17], which shows qualitatively the dynamic of variable linked to parameter

 DOI: https://doi.org/10.1590/1806-9126-RBEF-2020-0437

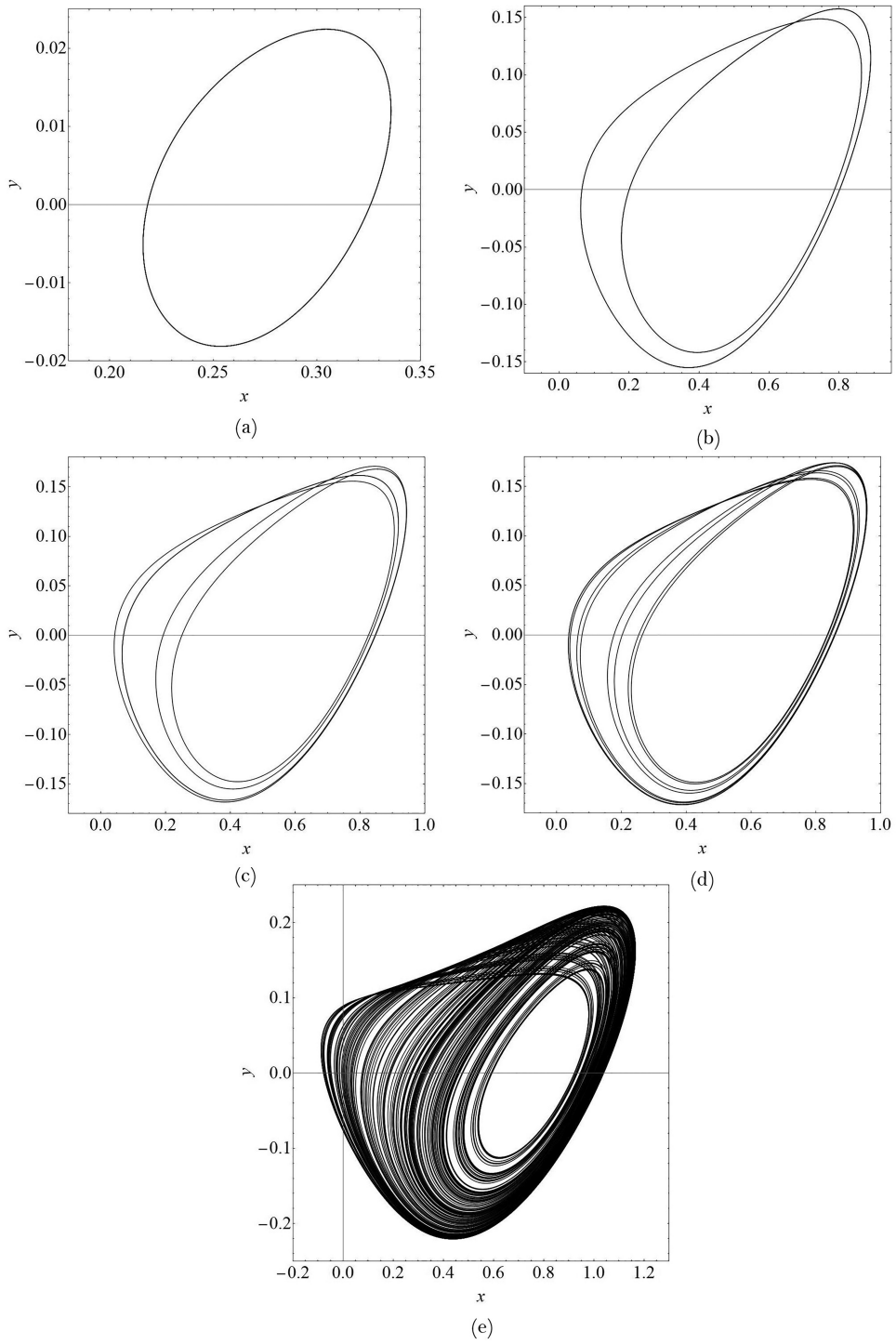

Figure 4: Period doubling sequence. (a) $|b| = \frac{5}{23}$, (b) $|b| = \frac{5}{12}$, (c) $|b| = \frac{5}{11.5}$, (d) $|b| = \frac{5}{11.38}$, (e) $|b| = \frac{5}{10}$.

variation. Figure 6 plots the system's attractor as function of $|b|$, for each parameter value an orbit x is generated starting from an random initial condition x_0. The plotted points are those obtained after a large number of iterations, that is, after the transient has decayed. Note that x reaches a steady state when the $|b|$ value is less than approximately 0.385, as indicated by the single branch. As $|b|$ increases, the branch splitting, yielding a period-2 cycle, i.e., period-doubling bifurcation occurs. When $|b| \approx 0.43$ the two branches splitting simultaneously, yielding a period-4 cycle. Increasing the $|b|$ still further produces a cascade of period-doubling, yielding period-8, period-16, and so on, until at $|b| \approx 0.44$, the map becomes chaotic. When $|b| > 0.44$ the orbit diagram reveals a mixture of chaos and order, with bands of periodic dynamics or "periodic windows" interspersed

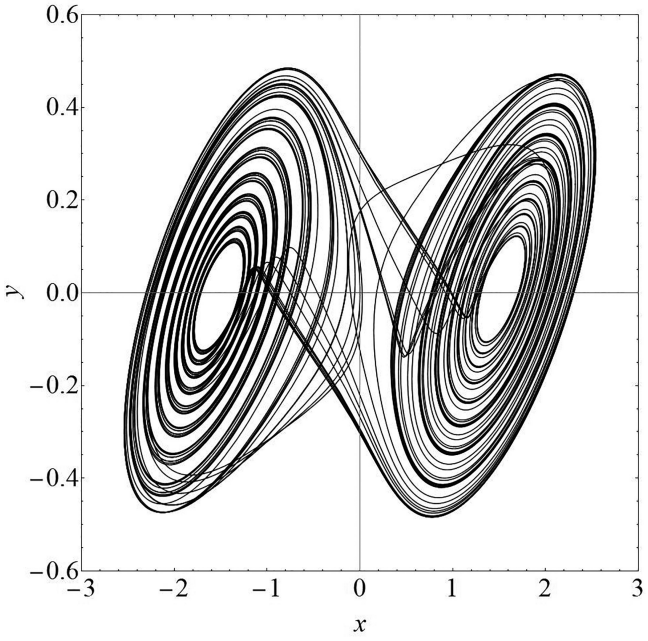

Figure 5: Double-scroll Chua atractor.

between chaotic regions. Periods 6, 5, 3, 4 correspond to large windows, the largest starting around $|b| \approx 0.465$ is the one containing a stable period-3 cycle, which splitting into a 2×3 period. A notable property of chaotic systems is the fine sensitivity to initial conditions. To show this the time-domain waveforms $w(\tau)$ for two trajectories are shown in Figure 7. These are two Chua's solutions generated using the same parameters as that of the double-scroll attractor of Figure 5. The initial conditions are as follows: $(x, y, z) = (0.001, 0.0, 0.04)$ for solid line, $(x, y, z) = (0.001, 0.0, 0.04001)$ for dotted line. That is, a variation between the initial conditions of 0.025% in just one component z. It is observed that trajectories diverge and become uncorrelated to approximately $\tau > 40$, that is, $t \approx 6\ ms$ when $R = 1.5\ k\Omega$ and $c_2 = 100\ nF$. Chaotic systems generally show this rapid decorrelation of orbits that originates from very close initial conditions, and this characteristic gives them an apparent randomness as well as the long-term unpredictability of the state.

A more accurate definition for sensitivity to initial conditions is that the divergence between neighboring trajectories is exponential. Let $\mathbf{x}_0(t)$ be a local point in trajectory at time t, and let a very close point be $\mathbf{x}_1(t) = \mathbf{x}_0(t) + \boldsymbol{\delta}(t)$. For a tiny deviation $\boldsymbol{\delta}(0)$ between initial conditions, the numerical analysis of chaotic attractors shows that growth of $\boldsymbol{\delta}(t)$ is such that $\boldsymbol{\delta}(t) \sim \boldsymbol{\delta}(0)e^{\lambda t}$. Where λ is defined as Lyapunov exponent, in unit (s^{-1}) for flows. For a three-dimensional continuous flow system like the Chua's oscillator we have $(\lambda_1,\ \lambda_2,\ \lambda_3)$. By definition the following order is established $\lambda_1 > \lambda_2 > \lambda_3$, with λ_1 being the largest Lyapunov exponent. A chaotic system requires that at least one exponent is positive, that is $\lambda_1 > 0$.

The initial deviation vector $\boldsymbol{\delta}(0)$ can also be seen as orthogonal axes in an ellipsoidal shape centered on the first point $\mathbf{x}_0$ of the orbit, the average rate of growth (per unit time) of the longest orthogonal axis of the ellipsoid shape is defined as the first Lyapunov number [18]. The solution of a variational equation then allows the calculation of how the variation $\boldsymbol{\delta}(t)$ evolves. This was the method used.

So for the chaotic system studied here we have the following final asymptotic values ($\lambda_1 = 0.14896$, $\lambda_2 = 0.00007$, $\lambda_3 = -3.64163$), the largest Lyapunov exponent is positive as expected. These exponents were calculated with dimensionless τ, the corresponding Lyapunov number is $\ln(\lambda_1)$, which means that the distance between the pair of points $\mathbf{x}_0(t)$ and $\mathbf{x}_1(t)$ that start out close together on the Chua attractor increases by the factor of ≈ 1.16 for each microsecond, on average. The discrepancy grows until a prediction of the future state becomes unacceptable within a certain tolerance k for the system, this occurs for a given time horizon that can be

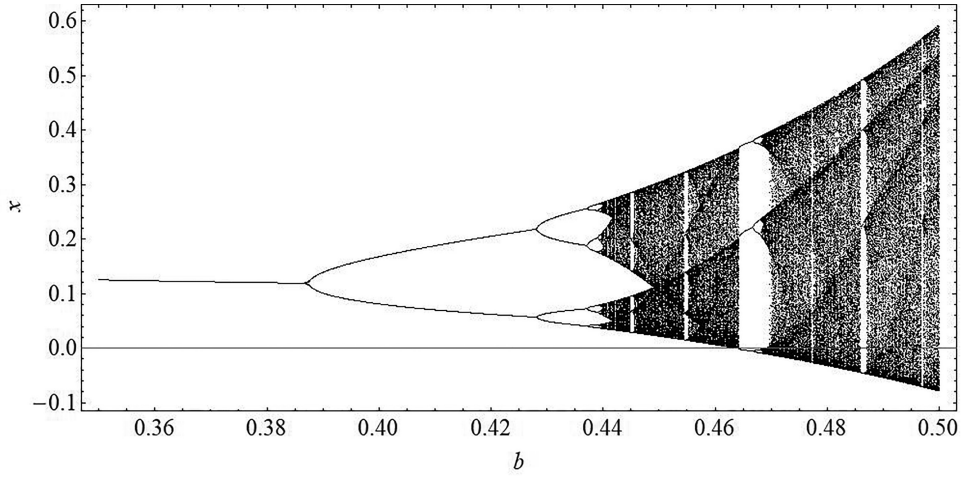

Figure 6: Orbit diagram.

 DOI: https://doi.org/10.1590/1806-9126-RBEF-2020-0437

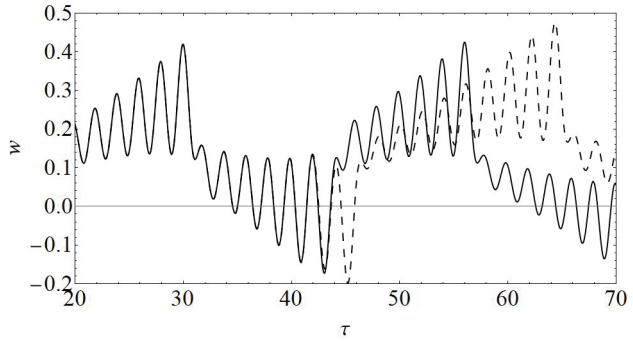

Figure 7: Wave-form $w(\tau)$. Sensitivity to initial conditions.

written [17]:

$$\tau_h \sim O\left(\frac{1}{\lambda_1}\ln\frac{k}{|\delta_0|}\right) \tag{6}$$

Considering $k = 10^{-3}$, for example, and assuming that an estimate for the initial state is within an uncertainty of $|\delta_0| = 10^{-8}$, then τ_h is,

$$\tau_h \approx 77.3$$

Now, if the measure of the initial state is improved about 1 million times so that $|\delta_0| = 10^{-14}$ and τ_h is,

$$\tau_h \approx 170.0$$

Therefore, although the measurement accuracy has been improved by 1 million times, the time horizon has been increased by only approximately 2 times, and this shows how difficult the long-term prediction for chaotic systems is.

Acknowledgments

I thank the reviewer for the helpful considerations.

References

[1] E.N. Lorenz, J. Atmos. Sci. **20**, 130 (1963).
[2] W. Ditto and T. Munakata, Communications of the ACM **38**, 96 (1995).
[3] L.O. Chua, Archiv für Elektronik und Übertragungstechnik **46**, 250 (1992).
[4] T. Matsumoto, IEEE Transactions on Circuits and Systems **31**, 1055 (1984).
[5] G.Q. Zhong and F. Ayrom, Circuit Theory and Applications **13**, 93 (1985).
[6] X. Rodet, Journal of Circuits, Systems and Computers **3**, 49 (1993).
[7] D. Romano, M. Bovati and F. Meloni, Int. J. Bif. and Chaos **9**, 1153 (1999).
[8] R. Tonelli and F. Meloni, Int. J. Bif. and Chaos **12**, 1451 (2002).
[9] J. Awrejcewicz and M.L. Calvisi, Int. J. Bif. and Chaos **12**, 671 (2002).
[10] W. Marszalek and H. Podhaisky, EPL **113**, 10005-p1 (2016).
[11] D. Jeltsema and A. D'oria-Cerezo, in Proceedings of 49th IEEE Conference on Decision and Control (CDC) (Institute of Electrical and Electronics Engineers (IEEE), Atlanta, 2010).
[12] L.O. Chua, IEICE Trans. Fundamentals **E76-A**, 704 (1993).
[13] L. Pivka, C.W. Wu and A. Huang, Journal of the Franklin Institute **331**, 705 (1994).
[14] M.P. Kennedy, IEEE Transactions on Circuits and Systems **40**, 640 (1993).
[15] M.P. Kennedy, IEEE Transactions on Circuits and Systems **40**, 657 (1993).
[16] R. Brown, Int. J. Bif. and Chaos. **2**, 889 (1992).
[17] S. Strogatz, *Non-linear Dynamics and Chaos. With Applications to Physics, Biology, Chemistry and Engineering* (Perseus Books, New York, 1994).
[18] K.T. Alligood, T.D. Sauer and J.A. Yorke. *Chaos: An introduction to dynamical systems* (Springer-Verlag, New York, 1996).